

Probing the scalar-induced gravitational waves with the Five-hundred-meter Aperture Spherical radio Telescope and the Square Kilometer Array

Jun Li,^{1,2,*} Guang-Hai Guo,^{1,†} and Yongcan Zu^{3,4,5,‡}

¹*School of Mathematics and Physics, Qingdao University of Science and Technology, Qingdao 266061, China*

²*CAS Key Laboratory of Theoretical Physics, Institute of Theoretical Physics, Chinese Academy of Sciences, Beijing 100190, China*

³*Key Laboratory of Marine Science and Numerical Modeling, First Institute of Oceanography, Ministry of Natural Resources, Qingdao, China*

⁴*Laboratory for Regional Oceanography and Numerical Modeling, Qingdao Marine Science and Technology Center, Qingdao, China*

⁵*Shandong Key Laboratory of Marine Science and Numerical Modeling, Qingdao, China*

(Dated: July 15, 2025)

Gravitational wave astronomy presents a promising opportunity to directly observe scalar-induced gravitational waves originating from the early universe. Future experiments, including ground-based interferometers like LIGO and Virgo, the Pulsar Timing Array, and telescopes such as FAST and SKA, are poised to significantly enhance sensitivity to these gravitational waves. In this paper, we combined Cosmic Microwave Background data with upper or lower limits of the stochastic gravitational wave background provided by FAST or SKA, to constrain scalar-induced gravitational waves. To provide a comprehensive forecast, we consider two scenarios: one where FAST or SKA does not detect scalar-induced gravitational waves, thereby setting an upper limit on the fractional energy density; and another where these waves are detected successfully, thus establishing a lower limit on the fractional energy density. In the Λ CDM+ r model, the scalar spectral index of the power-law power spectrum is constrained to $n_s = 0.9589^{+0.0021}_{-0.0011}$ from the combinations of CMB+BAO+SKA datasets in the upper limit scenario. The constraint shifts to $n_s = 0.9661^{+0.0027}_{-0.0039}$ in the lower limit scenario. Comparing with the constraint from the combinations of CMB+BAO datasets, the scalar spectral index n_s exhibits significant changes, which could serve as an indicator for detecting scalar-induced gravitational waves. In the Λ CDM+ α_s+r model and the Λ CDM+ $\alpha_s+\beta_s+r$ model, the running of the scalar spectral index α_s and the running of the scalar spectral index β_s also show notable variations, suggesting potential indicators. The numerical findings clearly demonstrate the impact of the upper and lower limits provided by FAST or SKA.

I. INTRODUCTION

Since the first direct detection of gravitational waves by the Laser Interferometer Gravitational-wave Observatory (LIGO) and Virgo detectors in 2015 [1], gravitational wave astronomy has rapidly advanced. Numerous detections have been made, including the landmark detection of both gravitational waves and electromagnetic signals from a neutron star merger in 2017 [2]. Future gravitational wave observatories, such as the Laser Interferometer Space Antenna (LISA) [3], will extend the sensitivity and frequency range of detections, allowing scientists to explore even more exotic and distant astrophysical phenomena. The Pulsar Timing Array (PTA) is an astronomical technique used to indirectly detect gravitational waves by observing an array of pulsars. Several notable PTAs include the Chinese PTA [4], the European PTA (EPTA) along with the Indian PTA [5, 6], the Parkes PTA (PPTA) [7, 8], and the North American Nanohertz Observatory for Gravitational Waves (NANOGrav) [9, 10]. Each of these collaborations contributes to the global effort of detecting gravitational waves through pulsar timing observations. In addition to telescopes such as the Five-hundred-meter Aperture Spherical radio Telescope (FAST) [11, 12] and the Square Kilometer Array (SKA) [12], all contribute to gravitational wave astronomy.

The detection of gravitational waves marks a pivotal milestone in astrophysics and cosmology, offering unprecedented opportunities to explore the early Universe and diverse astrophysical phenomena. This exploration notably includes a significant emphasis on primordial gravitational waves [13–28] and scalar-induced gravitational waves [29–88]. The scalar-induced gravitational waves are generated in the second order of perturbations. The curvature perturbations couple to the tensor perturbations at second-order which produce the induced gravitational waves in the radiation

*Electronic address: lijun@qust.edu.cn

†Electronic address: ghguo@qust.edu.cn

‡Electronic address: zuyongcan@fio.org.cn

dominated era. The evolution of induced gravitational waves in the radiation-dominated era was studied [29, 30]. As examples they computed the gravitational wave background generated by both a power-law spectrum on all scales, and a delta-function power spectrum on a single scale. The challenges associated with detecting scalar-induced gravitational waves are huge, which are second-order perturbations and inherently difficult to measure. Although the induced gravitational waves are suppressed by the square of curvature perturbations, but they can compare with primordial gravitational waves if the curvature perturbations are large enough. The enhancement of induced gravitational waves can be realized in some models [29–58]. Detecting scalar-induced gravitational waves is significance. The induced gravitational waves can serve as a direct window to probe the latest stages of inflation and as a probe of the very early universe prior to Big Bang Nucleosynthesis.

Both primordial gravitational waves and scalar-induced gravitational waves contribute to the generation of a stochastic gravitational wave background spanning a broad spectrum of frequency bands. Importantly, all these gravitational wave observations are sensitive to stochastic gravitational wave background. To achieve better constraints on primordial gravitational waves or scalar-induced gravitational waves, it is essential to combine observational datasets spanning different frequency bands. The LIGO and Virgo detectors, for instance, cover the high-frequency range from 20 Hz to 1726 Hz. LISA operates in the frequency range from 10^{-4} Hz to 1 Hz, while PTAs detect signals in the low-frequency range from 1.58×10^{-9} Hz to 8.27×10^{-7} Hz. Additionally, FAST spans frequencies from 6.34×10^{-10} Hz to 8.27×10^{-7} Hz, and SKA covers from 3.17×10^{-10} Hz to 8.27×10^{-7} Hz. Combining data from these different instruments across their respective frequency ranges holds the promise of providing deeper insights into the origins and nature of gravitational waves in our universe. In our previous study [25], we combined Cosmic Microwave Background (CMB) B-mode data from the BICEP2 and Keck array through 2015 season [89], along with the null search results of the stochastic gravitational wave background from LIGO and Virgo detectors, to establish the constraints on primordial gravitational waves. Additionally, we projected potential improvements using future gravitational wave experiments such as LISA, PTA, and FAST, by integrating their data with CMB B-mode polarization data.

In this context, our focus is on scalar-induced gravitational waves. According to observations by the Planck¹ satellite [90] and Baryon Acoustic Oscillation (BAO) measurements [91–93], the fractional energy density of scalar-induced gravitational waves around a frequency of 10^{-10} Hz is estimated to be approximately 10^{-17} . When comparing this estimate with the sensitivity curves for frequency and fractional energy density of detectors such as LIGO, Virgo, LISA, and PTA, it becomes evident that these instruments cannot effectively probe such minuscule scalar-induced gravitational waves. While the sensitivity curves of FAST and SKA are comparable, it is appropriate to consider the potential for these telescopes to constrain scalar-induced gravitational waves. To comprehensively forecast, we consider two scenarios: one where FAST or SKA cannot detect scalar-induced gravitational waves, constraining the fractional energy density by an upper limit. Alternatively, we explore a scenario where FAST or SKA can detect these waves, thereby constraining the fractional energy density by a lower limit. We combined CMB data from the Planck satellite [90], the BICEP and Keck Array through the 2018 Observing Season (BK18) [94], and Baryon Acoustic Oscillation (BAO) measurements [91–93], along with upper or lower limits of the stochastic gravitational wave background provided by FAST or SKA, to establish the constraints on scalar-induced gravitational waves.

II. THE SCALAR-INDUCED GRAVITATIONAL WAVES

In the conformal Newtonian gauge, the metric perturbation about the Friedmann-Robertson-Walker (FRW) background is typically expressed as

$$ds^2 = a^2 \left\{ -(1 + 2\Phi)d\eta^2 + \left[(1 - 2\Phi)\delta_{ij} + \frac{h_{ij}}{2} \right] dx^i dx^j \right\}, \quad (1)$$

where η denotes conformal time, $a(\eta)$ represents the scale factor of the FRW universe, Φ is the scalar perturbation representing the gravitational potential and h_{ij} represents the tensor perturbation, which is transverse and traceless. We neglect the vector perturbation, the first-order gravitational waves and the anisotropic stress. In the Fourier space, the tensor perturbation h_{ij} is expressed as

$$h_{ij}(\eta, \mathbf{x}) = \int \frac{d^3k}{(2\pi)^{3/2}} \left(e_{ij}^+(\mathbf{k}) h_{\mathbf{k}}^+(\eta) + e_{ij}^\times(\mathbf{k}) h_{\mathbf{k}}^\times(\eta) \right) e^{i\mathbf{k} \cdot \mathbf{x}}, \quad (2)$$

¹ Planck = TTTEEE+lowE+lensing

where the plus and cross polarization tensors can be expressed as

$$e_{ij}^+(\mathbf{k}) = \frac{1}{\sqrt{2}} \left(e_i(\mathbf{k})e_j(\mathbf{k}) - \bar{e}_i(\mathbf{k})\bar{e}_j(\mathbf{k}) \right), \quad e_{ij}^\times(\mathbf{k}) = \frac{1}{\sqrt{2}} \left(e_i(\mathbf{k})\bar{e}_j(\mathbf{k}) + \bar{e}_i(\mathbf{k})e_j(\mathbf{k}) \right), \quad (3)$$

the normalized vectors $e_i(\mathbf{k})$ and $\bar{e}_i(\mathbf{k})$ are mutually orthogonal and orthogonal to \mathbf{k} . The tensor equation of motion for h_{ij} can be straightforwardly derived from the perturbed Einstein equations up to second order. Scalar perturbations couple to tensor perturbations in the second-order equation. For this analysis, we also consider the propagation speed of scalar-induced gravitational waves within the framework of a FRW universe, and assume the speed of scalar-induced gravitational waves to be a constant parameter. The equation governing induced gravitational waves, with $\Phi_{\mathbf{k}}$ as the source, is given by

$$h_{\mathbf{k}}''(\eta) + 2\mathcal{H}h_{\mathbf{k}}'(\eta) + c_g^2 k^2 h_{\mathbf{k}}(\eta) = 4S_{\mathbf{k}}(\eta), \quad (4)$$

where the prime denotes derivative with respect to conformal time, $\mathcal{H} = a'/a = aH$ represents the conformal Hubble parameter, and c_g denotes the speed of scalar-induced gravitational waves. The source term is given by

$$S_{\mathbf{k}} = \int \frac{d^3q}{(2\pi)^{3/2}} e_{ij}(\mathbf{k})q_iq_j \left(2\Phi_{\mathbf{q}}\Phi_{\mathbf{k}-\mathbf{q}} + \frac{4}{3(1+\omega)} (\mathcal{H}^{-1}\Phi'_{\mathbf{q}} + \Phi_{\mathbf{q}}) (\mathcal{H}^{-1}\Phi'_{\mathbf{k}-\mathbf{q}} + \Phi_{\mathbf{k}-\mathbf{q}}) \right). \quad (5)$$

We consider the Green's function method as

$$h_{\mathbf{k}}(\eta) = \frac{4}{a(\eta)} \int_{\bar{\eta}}^{\eta} d\bar{\eta} G_{\mathbf{k}}(\eta, \bar{\eta}) a(\bar{\eta}) S_{\mathbf{k}}(\bar{\eta}), \quad (6)$$

where $G_{\mathbf{k}}(\eta, \bar{\eta})$ satisfies the equation

$$G_{\mathbf{k}}''(\eta, \bar{\eta}) + \left(c_g^2 k^2 - \frac{a''(\eta)}{a(\eta)} \right) G_{\mathbf{k}}(\eta, \bar{\eta}) = \delta(\eta - \bar{\eta}). \quad (7)$$

In the Radiation dominated Universe, the solution of the Green's function is

$$G_{\mathbf{k}}(\eta, \bar{\eta}) = \frac{1}{k} \sin[c_g k(\eta - \bar{\eta})]. \quad (8)$$

The power spectrum of scalar-induced gravitational waves is defined as

$$\langle h_{\mathbf{k}}(\eta) h_{\mathbf{k}'}(\eta) \rangle = \frac{2\pi^2}{k^3} \delta^{(3)}(\mathbf{k} + \mathbf{k}') \mathcal{P}_h(\eta, k), \quad (9)$$

and the fractional energy density is

$$\Omega_{\text{GW}}(\eta, k) = \frac{1}{24} \left(\frac{k}{aH} \right)^2 \overline{\mathcal{P}_h(\eta, k)}. \quad (10)$$

After calculation, the power spectrum of scalar-induced gravitational waves takes the form

$$\mathcal{P}_h(\eta, k) = 4 \int_0^\infty dv \int_{|1-v|}^{1+v} du \left(\frac{4v^2 - (1+v^2-u^2)^2}{4vu} \right)^2 I^2(v, u, x) \mathcal{P}_\zeta(kv) \mathcal{P}_\zeta(ku), \quad (11)$$

where $\mathcal{P}_\zeta(k)$ is the power spectrum of the primordial curvature perturbations, $x \equiv k\eta$, $u = |\mathbf{k} - \tilde{\mathbf{k}}|/k$ and $v = \tilde{k}/k$. The function $I(v, u, x)$ is defined as

$$I(v, u, x) = \int_0^x d\bar{x} \frac{a(\bar{\eta})}{a(\eta)} k G_{\mathbf{k}}(\eta, \bar{\eta}) f(v, u, \bar{x}), \quad (12)$$

where $\bar{x} \equiv k\bar{\eta}$, and $f(v, u, \bar{x})$ comes from the source term

$$\begin{aligned} f(v, u, \bar{x}) = & \frac{6(\omega+1)}{3\omega+5} \Phi(v\bar{x})\Phi(u\bar{x}) + \frac{6(1+3\omega)(\omega+1)}{(3\omega+5)^2} \left(\bar{x} \partial_{\bar{\eta}} \Phi(v\bar{x})\Phi(u\bar{x}) + \bar{x} \partial_{\bar{\eta}} \Phi(u\bar{x})\Phi(v\bar{x}) \right) \\ & + \frac{3(1+3\omega)^2(1+\omega)}{(3\omega+5)^2} \bar{x}^2 \partial_{\bar{\eta}} \Phi(v\bar{x}) \partial_{\bar{\eta}} \Phi(u\bar{x}). \end{aligned} \quad (13)$$

In the radiation-dominated Universe, the functions $f(v, u, \bar{x})$ and $I(v, u, x)$ can be written as our previous study [87].

For a power-law scalar power spectrum

$$\mathcal{P}_\zeta(k) = A_s \left(\frac{k}{k_*} \right)^{n_s - 1 + \frac{1}{2}\alpha_s \ln(k/k_*) + \frac{1}{6}\beta_s (\ln(k/k_*))^2}, \quad (14)$$

the power spectrum of scalar-induced gravitational waves is given by [87]

$$\mathcal{P}_h(\eta, k) = \frac{24Q(c_g, n_s, \alpha_s, \beta_s, k)}{(k\eta)^2} A_s^2 \left(\frac{k}{k_*} \right)^{2[n_s - 1 + \frac{1}{2}\alpha_s \ln(k/k_*) + \frac{1}{6}\beta_s (\ln(k/k_*))^2]}, \quad (15)$$

where A_s represents the scalar amplitude of the power-law power spectrum at the pivot scale $k_* = 0.05 \text{ Mpc}^{-1}$, n_s denotes the scalar spectral index, $\alpha_s \equiv dn_s/d \ln k$ represents the running of the scalar spectral index, $\beta_s \equiv d^2 n_s / d \ln k^2$ indicates the running of the running of the scalar spectral index, and $Q(c_g, n_s, \alpha_s, \beta_s, k)$ are the overall coefficients which depend on c_g , n_s , α_s , β_s and k , and can be found in Table 4 of [87]. The connection between the parameters of power-law spectrum and scalar-induced gravitational waves is established. The fractional energy density becomes

$$\Omega_{\text{GW}}(\eta, k) = Q(c_g, n_s, \alpha_s, \beta_s, k) A_s^2 \left(\frac{k}{k_*} \right)^{2[n_s - 1 + \frac{1}{2}\alpha_s \ln(k/k_*) + \frac{1}{6}\beta_s (\ln(k/k_*))^2]}. \quad (16)$$

Here, we investigate the scalar-induced gravitational waves propagating at the speed of light first. According to Planck+BAO observations [90], the central values are $n_s = 0.9647 \pm 0.0043$, $\alpha_s = 0.009 \pm 0.012$ and $\beta_s = 0.0011 \pm 0.0099$. The strength of the scalar-induced gravitational waves around the frequency of 10^{-10} Hz would be of the order 10^{-17} .

The gravitational-wave detections also show the sensitivity curves of frequency and Ω_{GW} in the detectible ranges which can be used to find scalar-induced gravitational waves. To comprehensively forecast, we consider two scenarios: one where gravitational-wave detections cannot detect scalar-induced gravitational waves, constraining the fractional energy density by an upper limit. Alternatively, we explore a scenario where gravitational-wave detections can detect scalar-induced gravitational waves, thereby constraining the fractional energy density by a lower limit. Combining these limits with Eq. (16), we can obtain the constraints on the power spectrum of the primordial curvature perturbations. Comparing with LIGO, Virgo, LISA, and PTA detectors, the sensitivity curve of FAST and the energy density fraction Ω_{GW} of the scalar-induced gravitational waves would intersect around the frequency of $3 * 10^{-9} \text{ Hz}$ which exhibits in Figure 3 of [85]. According to the sensitivity curve of FAST, the strength of the scalar-induced gravitational waves around the frequency of $6.34 * 10^{-10} \text{ Hz}$ would be of the order 10^{-19} [12]. As the parameters of power-law spectrum influence the fractional energy density, they are sensitive to the upper or lower limit of FAST. So we could expect that the sensitivity curve of FAST leads to distinct constraints on the parameters of power-law spectrum.

III. THE CONSTRAINTS ON SCALAR-INDUCED GRAVITATIONAL WAVES FROM THE COMBINATIONS OF CMB+BAO WITH UPPER OR LOWER LIMITS PROVIDED BY FAST OR SKA

In the standard ΛCDM model, the six parameters are the baryon density parameter $\Omega_b h^2$, the cold dark matter density $\Omega_c h^2$, the angular size of the horizon at the last scattering surface θ_{MC} , the optical depth τ , the scalar amplitude A_s and the scalar spectral index n_s . In the literature, the tensor-to-scalar ratio r is utilized to quantify the tensor amplitude A_t relative to the scalar amplitude A_s at the pivot scale, namely

$$r \equiv \frac{A_t}{A_s}. \quad (17)$$

We use the publicly available Cosmomic code [95] to extend the standard ΛCDM model by incorporating parameters such as the tensor-to-scalar ratio r , the running of the scalar spectral index α_s , and the running of the running of the scalar spectral index β_s . These parameters are constrained using the combinations of CMB²+BAO, along with the upper or lower limits of the stochastic gravitational wave background provided by FAST or SKA. The numerical results are presented in Tables I to III, and Figures 1 to 3.

² CMB=Planck+BK18

Parameter	CMB+BAO	CMB+BAO+SKA(upper limit)	CMB+BAO+SKA(lower limit)
$\Omega_b h^2$	0.02241 ± 0.00013	0.02233 ± 0.00013	0.02242 ± 0.00013
$\Omega_c h^2$	0.11954 ± 0.00091	0.12056 ± 0.00079	$0.11942^{+0.00087}_{-0.00088}$
$100\theta_{\text{MC}}$	1.04099 ± 0.00029	$1.04088^{+0.00027}_{-0.00028}$	1.04101 ± 0.00028
τ	$0.0567^{+0.0070}_{-0.0071}$	$0.0505^{+0.0063}_{-0.0062}$	$0.0572^{+0.0066}_{-0.0076}$
$\ln(10^{10} A_s)$	3.049 ± 0.014	3.038 ± 0.013	3.049 ± 0.014
n_s	0.9654 ± 0.0037	$0.9589^{+0.0021}_{-0.0011}$	$0.9661^{+0.0027}_{-0.0039}$
$r_{0.05}$ (95% CL)	< 0.038	< 0.035	< 0.039

TABLE I: The 68% confidence limits on the cosmological parameters in the $\Lambda\text{CDM}+r$ model are derived from the combinations of CMB+BAO, CMB+BAO+SKA(upper limit), and CMB+BAO+SKA(lower limit) datasets, respectively.

Parameter	CMB+BAO	CMB+BAO+SKA(upper limit)	CMB+BAO+SKA(lower limit)
$\Omega_b h^2$	0.02239 ± 0.00015	0.02245 ± 0.00014	$0.02236^{+0.00013}_{-0.00014}$
$\Omega_c h^2$	$0.11955^{+0.00093}_{-0.00094}$	$0.11960^{+0.00092}_{-0.00094}$	$0.11949^{+0.00093}_{-0.00094}$
$100\theta_{\text{MC}}$	$1.04099^{+0.00030}_{-0.00029}$	$1.04100^{+0.00029}_{-0.00028}$	$1.04098^{+0.00030}_{-0.00029}$
τ	$0.0563^{+0.0069}_{-0.0078}$	$0.0578^{+0.0070}_{-0.0076}$	$0.0554^{+0.0070}_{-0.0076}$
$\ln(10^{10} A_s)$	$3.048^{+0.015}_{-0.014}$	3.052 ± 0.014	$3.045^{+0.014}_{-0.015}$
n_s	0.9656 ± 0.0039	0.9643 ± 0.0038	0.9664 ± 0.0038
α_s	$0.0015^{+0.0079}_{-0.0080}$	$-0.0062^{+0.0056}_{-0.0023}$	$0.0066^{+0.0030}_{-0.0069}$
$r_{0.05}$ (95% CL)	< 0.037	< 0.039	< 0.037

TABLE II: The 68% confidence limits on the cosmological parameters in the $\Lambda\text{CDM}+\alpha_s+r$ model are derived from the combinations of CMB+BAO, CMB+BAO+SKA(upper limit), and CMB+BAO+SKA(lower limit) datasets, respectively.

In the $\Lambda\text{CDM}+r$ model, the scalar spectral index is constrained to $n_s = 0.9589^{+0.0021}_{-0.0011}$ from the combinations of CMB+BAO+SKA datasets in the upper limit scenario. The constraint shifts to $n_s = 0.9661^{+0.0027}_{-0.0039}$ in the lower limit scenario. When compared to the constraint from the combinations of CMB+BAO datasets alone, the scalar spectral index n_s shows notable changes, suggesting its potential role as an indicator for detecting scalar-induced gravitational waves. Detailed values are provided in Table I. The contour plots and likelihood distributions of cosmological parameters from the combinations of CMB+BAO+SKA(lower limit) datasets remain largely consistency with those derived from CMB+BAO, except for n_s . While the contour plots and likelihood distributions from the combinations of CMB+BAO+SKA(upper limit) datasets noticeably differ from those of CMB+BAO, as depicted in Figure 1. The numerical findings clearly demonstrate the significant influence of the upper and lower limits provided by SKA.

In the $\Lambda\text{CDM}+\alpha_s+r$ model, the scalar spectral index and the running of the scalar spectral index are constrained to $n_s = 0.9643 \pm 0.0038$ and $\alpha_s = -0.0062^{+0.0056}_{-0.0023}$, respectively, from the combinations of CMB+BAO+SKA datasets in the upper limit scenario. The constraints shift to $n_s = 0.9664 \pm 0.0038$ and $\alpha_s = 0.0066^{+0.0030}_{-0.0069}$ in the lower limit scenario. Comparison with constraints from the combinations of CMB+BAO datasets reveals notable changes in α_s .

Parameter	CMB+BAO	CMB+BAO+FAST(upper limit)	CMB+BAO+FAST(lower limit)
$\Omega_b h^2$	0.02241 ± 0.00015	0.02243 ± 0.00014	0.02239 ± 0.00014
$\Omega_c h^2$	0.11950 ± 0.00096	$0.11936^{+0.00093}_{-0.00094}$	$0.11958^{+0.00093}_{-0.00091}$
$100\theta_{\text{MC}}$	1.04098 ± 0.00029	1.04099 ± 0.00029	1.04100 ± 0.00029
τ	$0.0546^{+0.0075}_{-0.0088}$	$0.0528^{+0.0073}_{-0.0072}$	$0.0586^{+0.0075}_{-0.0085}$
$\ln(10^{10} A_s)$	$3.044^{+0.015}_{-0.017}$	3.041 ± 0.015	$3.052^{+0.015}_{-0.017}$
n_s	0.9668 ± 0.0053	$0.9690^{+0.0046}_{-0.0050}$	$0.9635^{+0.0046}_{-0.0042}$
α_s	-0.0016 ± 0.011	$-0.0065^{+0.010}_{-0.009}$	0.0067 ± 0.009
β_s	-0.0083 ± 0.023	$-0.0223^{+0.020}_{-0.009}$	$0.0149^{+0.006}_{-0.016}$
$r_{0.05}$ (95% CL)	< 0.036	< 0.037	< 0.037

TABLE III: The 68% confidence limits on the cosmological parameters in the $\Lambda\text{CDM}+\alpha_s+\beta_s+r$ model are derived from the combinations of CMB+BAO, CMB+BAO+FAST(upper limit), and CMB+BAO+FAST(lower limit) datasets, respectively.

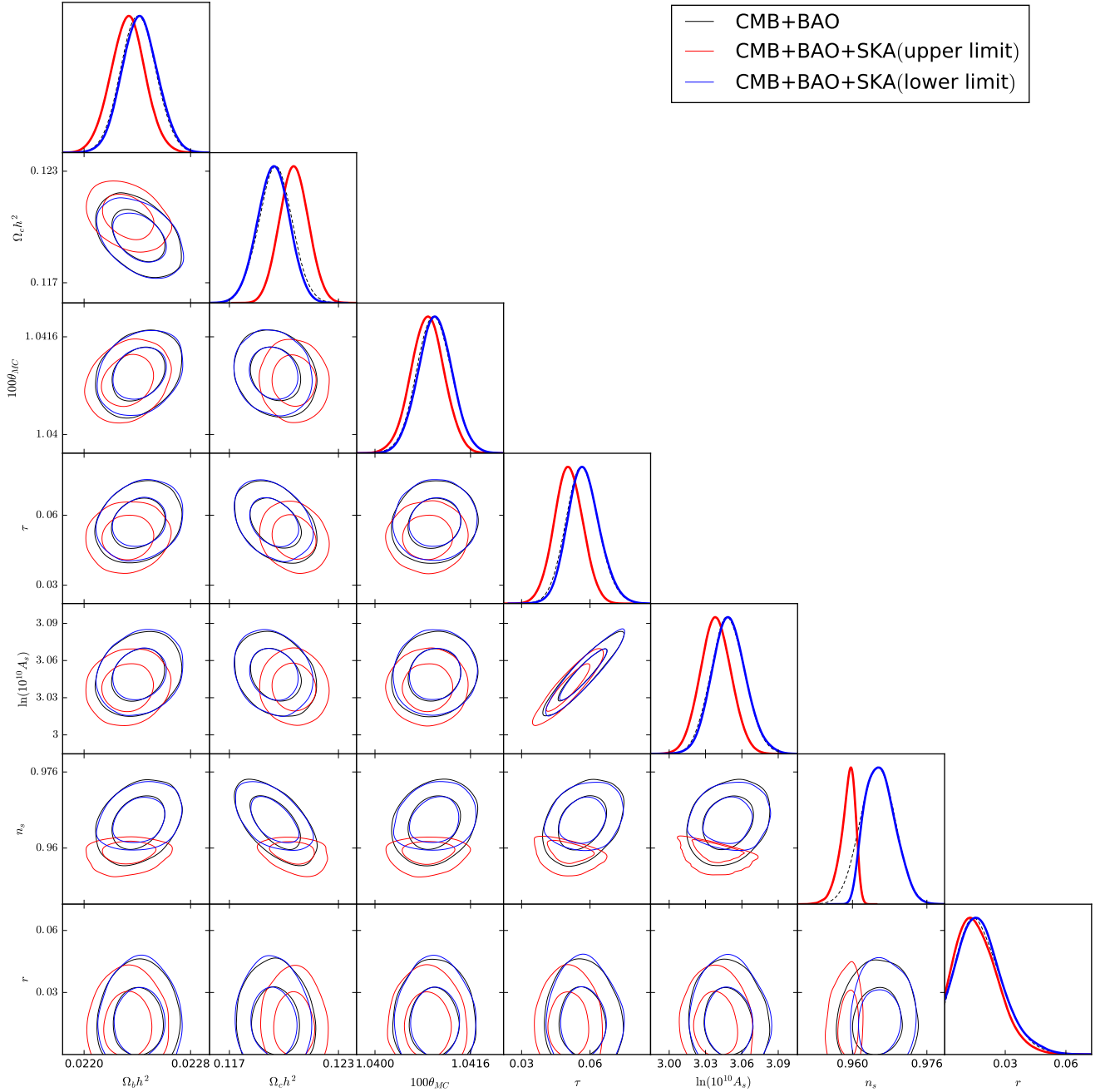


FIG. 1: The contour plots and likelihood distributions of cosmological parameters in the $\Lambda\text{CDM}+r$ model are shown at the 68% and 95% confidence levels, derived from the combinations of CMB+BAO, CMB+BAO+SKA(upper limit), and CMB+BAO+SKA(lower limit) datasets, respectively. The filled lines in the likelihood distributions represent the constraints from CMB+BAO+SKA datasets. The dashed lines in the likelihood distributions represent the constraints from CMB+BAO datasets.

Detailed values can be found in Table II. The contour plots and likelihood distributions of α_s indicate a predominantly positive constraint in the lower limit scenario, whereas the constraints lean negative in the upper limit scenario, as depicted in Figure 2.

In the $\Lambda\text{CDM}+\alpha_s+\beta_s+r$ model, the parameters describing the scalar spectral index, the running of the scalar spectral index, and the running of the running of the scalar spectral index are constrained as follows: in the upper limit scenario, $n_s = 0.9690^{+0.0046}_{-0.0050}$, $\alpha_s = -0.0065^{+0.010}_{-0.009}$, and $\beta_s = -0.0223^{+0.020}_{-0.009}$, derived from combined CMB+BAO+FAST datasets. The values shift to $n_s = 0.9635^{+0.0046}_{-0.0042}$, $\alpha_s = 0.0067 \pm 0.009$, and $\beta_s = 0.0149^{+0.006}_{-0.016}$ in the lower limit

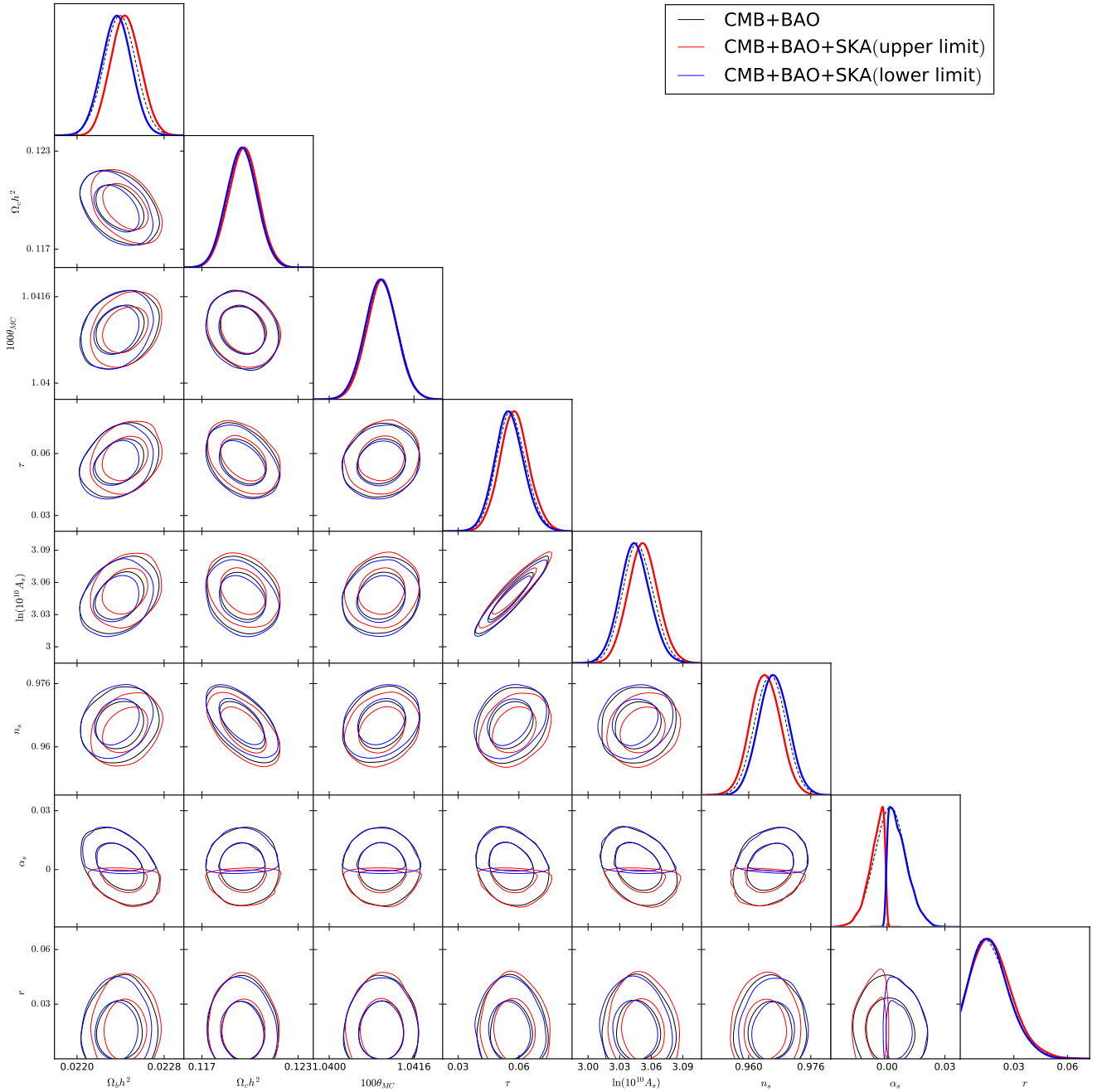


FIG. 2: The contour plots and likelihood distributions of cosmological parameters in the $\Lambda\text{CDM} + \alpha_s + r$ model are shown at the 68% and 95% confidence levels, derived from the combinations of CMB+BAO, CMB+BAO+SKA(upper limit), and CMB+BAO+SKA(lower limit) datasets, respectively. The filled lines in the likelihood distributions represent the constraints from CMB+BAO+SKA datasets. The dashed lines in the likelihood distributions represent the constraints from CMB+BAO datasets.

scenario. Comparative analysis with constraints solely from CMB+BAO datasets demonstrates significant variations, particularly in α_s and β_s . Detailed numerical values are summarized in Table III. The contour plots and likelihood distributions of β_s illustrate predominantly positive constraints in the lower limit scenario, whereas they lean negative in the upper limit scenario, as depicted in Figure 3. The findings underscore the significant impact of upper and lower limits provided by FAST. In the $\Lambda\text{CDM} + \alpha_s + r$ model and the $\Lambda\text{CDM} + \alpha_s + \beta_s + r$ model, the running of the scalar spectral index α_s and the running of the running of the scalar spectral index β_s exhibit notable variations, indicating potential observational insights.

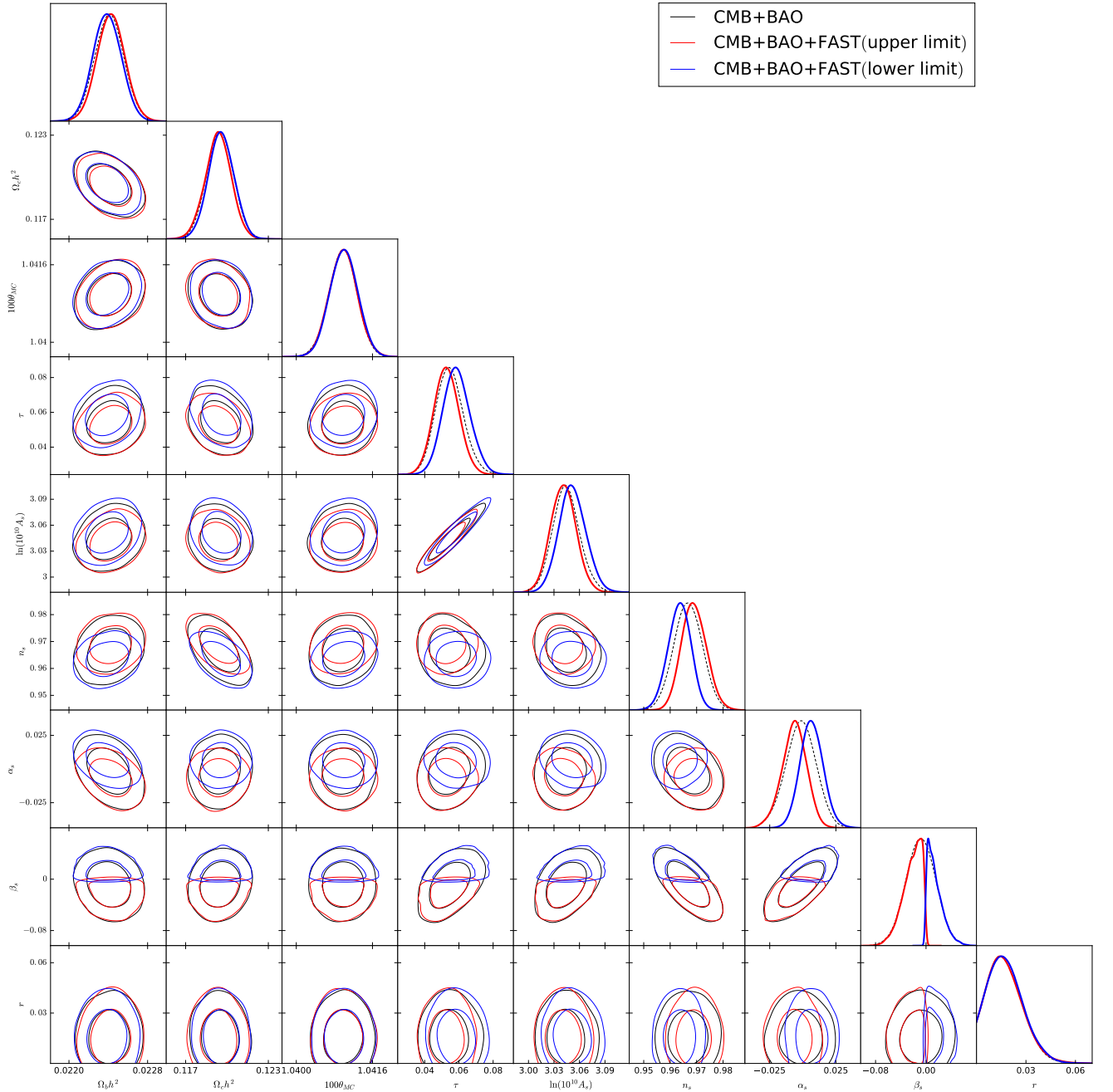


FIG. 3: The contour plots and likelihood distributions of cosmological parameters in the $\Lambda\text{CDM} + \alpha_s + \beta_s + r$ model are shown at the 68% and 95% confidence levels, derived from the combinations of CMB+BAO, CMB+BAO+FAST(upper limit), and CMB+BAO+FAST(lower limit) datasets, respectively. The filled lines in the likelihood distributions represent the constraints from CMB+BAO+FAST datasets. The dashed lines in the likelihood distributions represent the constraints from CMB+BAO datasets.

IV. SUMMARY

Scalar-induced gravitational waves originating from the early universe are a key prediction of various inflationary models where quantum fluctuations during inflation can generate a stochastic background of gravitational waves. These waves imprint specific signatures in the polarization of CMB and in the large-scale structure of the universe. The signatures offer complementary observational avenues to confirm their existence and investigate their properties. Detecting scalar-induced gravitational waves requires highly sensitive instruments capable of measuring minute

distortions in spacetime.

In this paper, we combined CMB data with upper or lower limits of the stochastic gravitational wave background provided by FAST or SKA, to constrain scalar-induced gravitational waves. In the Λ CDM+ r model, the scalar spectral index of the power-law power spectrum is constrained to $n_s = 0.9589^{+0.0021}_{-0.0011}$ in the upper limit scenario, derived from combined CMB+BAO+SKA datasets. In the lower limit scenario, this constraint shifts to $n_s = 0.9661^{+0.0027}_{-0.0039}$. These constraints represent significant deviations from those obtained using CMB+BAO datasets alone, suggesting n_s as a potential indicator for detecting scalar-induced gravitational waves. In the Λ CDM+ α_s+r model and the Λ CDM+ $\alpha_s+\beta_s+r$ model, the running of the scalar spectral index α_s and the running of the running of the scalar spectral index β_s also exhibit notable variations. These parameters further underscore the sensitivity of cosmological constraints to gravitational wave signatures, particularly influenced by the upper and lower limits provided by facilities like FAST or SKA. These numerical results emphasize the critical role of future observatories in refining our understanding of early universe physics through precise measurements of n_s , α_s , and β_s from combined datasets. Such advancements promise to deepen our insights into the origin and evolution of the cosmos.

Acknowledgments. Jun Li is supported by the National Natural Science Foundation of China (Grant No. 12405069), the Natural Science Foundation of Shandong Province (Grant No. ZR2021QA073) and Research Start-up Fund of QUST (Grant No. 1203043003587). Yongcan Zu is supported by the Basic Scientific Fund for National Public Research Institutes of China (No. 2025Q04).

-
- [1] B. P. Abbott *et al.* [LIGO Scientific and Virgo], Phys. Rev. Lett. **116** (2016) no.6, 061102 [arXiv:1602.03837 [gr-qc]].
 - [2] B. P. Abbott *et al.* [LIGO Scientific and Virgo], Phys. Rev. Lett. **119** (2017) no.16, 161101 [arXiv:1710.05832 [gr-qc]].
 - [3] C. Caprini, M. Hindmarsh, S. Huber, T. Konstandin, J. Kozaczuk, G. Nardini, J. M. No, A. Petiteau, P. Schwaller and G. Servant, *et al.* JCAP **04** (2016), 001 [arXiv:1512.06239 [astro-ph.CO]].
 - [4] H. Xu, S. Chen, Y. Guo, J. Jiang, B. Wang, J. Xu, Z. Xue, R. N. Caballero, J. Yuan and Y. Xu, *et al.* Res. Astron. Astrophys. **23** (2023) no.7, 075024 [arXiv:2306.16216 [astro-ph.HE]].
 - [5] J. Antoniadis *et al.* [EPTA], Astron. Astrophys. **678** (2023), A48 [arXiv:2306.16224 [astro-ph.HE]].
 - [6] J. Antoniadis *et al.* [EPTA and InPTA], Astron. Astrophys. **678** (2023), A50 [arXiv:2306.16214 [astro-ph.HE]].
 - [7] A. Zic, D. J. Reardon, A. Kapur, G. Hobbs, R. Mandow, M. Curylo, R. M. Shannon, J. Askew, M. Bailes and N. D. R. Bhat, *et al.* Publ. Astron. Soc. Austral. **40** (2023), e049 [arXiv:2306.16230 [astro-ph.HE]].
 - [8] D. J. Reardon, A. Zic, R. M. Shannon, G. B. Hobbs, M. Bailes, V. Di Marco, A. Kapur, A. F. Rogers, E. Thrane and J. Askew, *et al.* Astrophys. J. Lett. **951** (2023) no.1, L6 [arXiv:2306.16215 [astro-ph.HE]].
 - [9] G. Agazie *et al.* [NANOGrav], Astrophys. J. Lett. **951** (2023) no.1, L8 [arXiv:2306.16213 [astro-ph.HE]].
 - [10] G. Agazie *et al.* [NANOGrav], Astrophys. J. Lett. **951** (2023) no.1, L9 doi:10.3847/2041-8213/acda9a [arXiv:2306.16217 [astro-ph.HE]].
 - [11] R. Nan, D. Li, C. Jin, Q. Wang, L. Zhu, W. Zhu, H. Zhang, Y. Yue and L. Qian, Int. J. Mod. Phys. D **20** (2011), 989-1024 [arXiv:1105.3794 [astro-ph.IM]].
 - [12] K. Kuroda, W. T. Ni and W. P. Pan, Int. J. Mod. Phys. D **24** (2015) no.14, 1530031 [arXiv:1511.00231 [gr-qc]].
 - [13] Y. F. Cai, C. Lin, B. Wang and S. F. Yan, Phys. Rev. Lett. **126** (2021) no.7, 071303 [arXiv:2009.09833 [gr-qc]].
 - [14] W. Lin and M. Ishak, Phys. Rev. D **94** (2016) no.12, 123011 [arXiv:1605.03504 [astro-ph.CO]].
 - [15] P. Brax, S. Céspedes and A. C. Davis, JCAP **03** (2018), 008 [arXiv:1710.09818 [astro-ph.CO]].
 - [16] W. Giarè and F. Renzi, Phys. Rev. D **102** (2020) no.8, 083530 [arXiv:2007.04256 [astro-ph.CO]].
 - [17] Y. Cai, Y. T. Wang and Y. S. Piao, Phys. Rev. D **94** (2016) no.4, 043002 [arXiv:1602.05431 [astro-ph.CO]].
 - [18] J. M. Ezquiaga, W. Hu, M. Lagos and M. X. Lin, JCAP **11** (2021) no.11, 048 [arXiv:2108.10872 [astro-ph.CO]].
 - [19] S. Dubovsky, R. Flauger, A. Starobinsky and I. Tkachev, Phys. Rev. D **81** (2010), 023523 [arXiv:0907.1658 [astro-ph.CO]].
 - [20] P. Campeti, E. Komatsu, D. Poletti and C. Baccigalupi, JCAP **01** (2021), 012 [arXiv:2007.04241 [astro-ph.CO]].
 - [21] K. Saikawa and S. Shirai, JCAP **05** (2018), 035 [arXiv:1803.01038 [hep-ph]].
 - [22] J. Li and Q. G. Huang, JCAP **02** (2018), 020 [arXiv:1712.07771 [astro-ph.CO]].
 - [23] J. Li and Q. G. Huang, Eur. Phys. J. C **78** (2018) no.11, 980 [arXiv:1806.01440 [astro-ph.CO]].
 - [24] J. Li and Q. G. Huang, Sci. China Phys. Mech. Astron. **62** (2019) no.12, 120412 [arXiv:1906.01336 [astro-ph.CO]].
 - [25] J. Li, Z. C. Chen and Q. G. Huang, Sci. China Phys. Mech. Astron. **62** (2019) no.11, 110421 [arXiv:1907.09794 [astro-ph.CO]].
 - [26] J. Li and G. H. Guo, Mod. Phys. Lett. A **37** (2022) no.10, 2250066 [arXiv:2101.07970 [astro-ph.CO]].
 - [27] J. Li, G. H. Guo and Y. Zu, Mod. Phys. Lett. A **39** (2024) no.07, 2450019
 - [28] J. Li, Universe **8** (2022) no.7, 367 [arXiv:2110.14913 [astro-ph.CO]].
 - [29] K. N. Ananda, C. Clarkson and D. Wands, Phys. Rev. D **75** (2007), 123518 [arXiv:gr-qc/0612013 [gr-qc]].
 - [30] D. Baumann, P. J. Steinhardt, K. Takahashi and K. Ichiki, Phys. Rev. D **76** (2007), 084019 [arXiv:hep-th/0703290 [hep-th]].
 - [31] K. Inomata, M. Kawasaki, K. Mukaida, Y. Tada and T. T. Yanagida, Phys. Rev. D **95** (2017) no.12, 123510 [arXiv:1611.06130 [astro-ph.CO]].
 - [32] K. Kohri and T. Terada, Phys. Rev. D **97** (2018) no.12, 123532 [arXiv:1804.08577 [gr-qc]].
 - [33] Y. Lu, Y. Gong, Z. Yi and F. Zhang, JCAP **12** (2019), 031 [arXiv:1907.11896 [gr-qc]].

- [34] L. Alabidi, K. Kohri, M. Sasaki and Y. Sendouda, JCAP **09** (2012), 017 [arXiv:1203.4663 [astro-ph.CO]].
- [35] C. Unal, Phys. Rev. D **99** (2019) no.4, 041301 [arXiv:1811.09151 [astro-ph.CO]].
- [36] L. Alabidi, K. Kohri, M. Sasaki and Y. Sendouda, JCAP **05** (2013), 033 [arXiv:1303.4519 [astro-ph.CO]].
- [37] H. Di and Y. Gong, JCAP **07** (2018), 007 [arXiv:1707.09578 [astro-ph.CO]].
- [38] W. T. Xu, J. Liu, T. J. Gao and Z. K. Guo, Phys. Rev. D **101** (2020) no.2, 023505 [arXiv:1907.05213 [astro-ph.CO]].
- [39] Z. Zhou, J. Jiang, Y. F. Cai, M. Sasaki and S. Pi, Phys. Rev. D **102** (2020) no.10, 103527 [arXiv:2010.03537 [astro-ph.CO]].
- [40] K. Inomata and T. Nakama, Phys. Rev. D **99** (2019) no.4, 043511 [arXiv:1812.00674 [astro-ph.CO]].
- [41] K. Inomata, K. Kohri, T. Nakama and T. Terada, Phys. Rev. D **100** (2019), 043532 [arXiv:1904.12879 [astro-ph.CO]].
- [42] K. Inomata, K. Kohri, T. Nakama and T. Terada, JCAP **10** (2019), 071 [arXiv:1904.12878 [astro-ph.CO]].
- [43] Z. C. Chen, C. Yuan and Q. G. Huang, Phys. Rev. Lett. **124** (2020) no.25, 251101 [arXiv:1910.12239 [astro-ph.CO]].
- [44] C. Yuan, Z. C. Chen and Q. G. Huang, Phys. Rev. D **101** (2020) no.4, 043019 [arXiv:1910.09099 [astro-ph.CO]].
- [45] H. Assadullahi and D. Wands, Phys. Rev. D **81** (2010), 023527 [arXiv:0907.4073 [astro-ph.CO]].
- [46] H. Assadullahi and D. Wands, Phys. Rev. D **79** (2009), 083511 [arXiv:0901.0989 [astro-ph.CO]].
- [47] R. G. Cai, S. Pi, S. J. Wang and X. Y. Yang, JCAP **05** (2019), 013 [arXiv:1901.10152 [astro-ph.CO]].
- [48] R. G. Cai, S. Pi, S. J. Wang and X. Y. Yang, JCAP **10** (2019), 059 [arXiv:1907.06372 [astro-ph.CO]].
- [49] R. g. Cai, S. Pi and M. Sasaki, Phys. Rev. Lett. **122** (2019) no.20, 201101 [arXiv:1810.11000 [astro-ph.CO]].
- [50] Y. F. Cai, C. Chen, X. Tong, D. G. Wang and S. F. Yan, Phys. Rev. D **100** (2019) no.4, 043518 [arXiv:1902.08187 [astro-ph.CO]].
- [51] M. Giovannini, Phys. Rev. D **82** (2010), 083523 [arXiv:1008.1164 [astro-ph.CO]].
- [52] S. Matarrese, S. Mollerach and M. Bruni, Phys. Rev. D **58** (1998), 043504 [arXiv:astro-ph/9707278 [astro-ph]].
- [53] H. Noh and J. c. Hwang, Phys. Rev. D **69** (2004), 104011 [arXiv:astro-ph/0305123 [astro-ph]].
- [54] B. Osano, C. Pitrou, P. Dunsby, J. P. Uzan and C. Clarkson, JCAP **04** (2007), 003 [arXiv:gr-qc/0612108 [gr-qc]].
- [55] N. Orlofsky, A. Pierce and J. D. Wells, Phys. Rev. D **95** (2017) no.6, 063518 [arXiv:1612.05279 [astro-ph.CO]].
- [56] J. R. Espinosa, D. Racco and A. Riotto, JCAP **09** (2018), 012 [arXiv:1804.07732 [hep-ph]].
- [57] N. Bartolo, V. De Luca, G. Franciolini, M. Peloso, D. Racco and A. Riotto, Phys. Rev. D **99** (2019) no.10, 103521 [arXiv:1810.12224 [astro-ph.CO]].
- [58] Y. Tada and S. Yokoyama, Phys. Rev. D **100** (2019) no.2, 023537 [arXiv:1904.10298 [astro-ph.CO]].
- [59] Z. Q. You, Z. Yi and Y. Wu, JCAP **11** (2023), 065 [arXiv:2307.04419 [gr-qc]].
- [60] J. H. Jin, Z. C. Chen, Z. Yi, Z. Q. You, L. Liu and Y. Wu, JCAP **09** (2023), 016 [arXiv:2307.08687 [astro-ph.CO]].
- [61] G. Domènech and M. Sasaki, Phys. Rev. D **103** (2021) no.6, 063531 [arXiv:2012.14016 [gr-qc]].
- [62] J. C. Hwang, D. Jeong and H. Noh, Astrophys. J. **842** (2017) no.1, 46 [arXiv:1704.03500 [astro-ph.CO]].
- [63] K. Inomata and T. Terada, Phys. Rev. D **101** (2020) no.2, 023523 [arXiv:1912.00785 [gr-qc]].
- [64] K. Tomikawa and T. Kobayashi, Phys. Rev. D **101** (2020) no.8, 083529 [arXiv:1910.01880 [gr-qc]].
- [65] Z. Yi, Y. Gong, B. Wang and Z. h. Zhu, Phys. Rev. D **103** (2021) no.6, 063535 [arXiv:2007.09957 [gr-qc]].
- [66] G. Domènech, S. Pi and M. Sasaki, JCAP **08** (2020), 017 [arXiv:2005.12314 [gr-qc]].
- [67] F. Hajkarim and J. Schaffner-Bielich, Phys. Rev. D **101** (2020) no.4, 043522 [arXiv:1910.12357 [hep-ph]].
- [68] S. Pi and M. Sasaki, JCAP **09** (2020), 037 [arXiv:2005.12306 [gr-qc]].
- [69] C. Yuan, Z. C. Chen and Q. G. Huang, Phys. Rev. D **100** (2019) no.8, 081301 [arXiv:1906.11549 [astro-ph.CO]].
- [70] C. Yuan, Z. C. Chen and Q. G. Huang, Phys. Rev. D **101** (2020) no.6, 063018 [arXiv:1912.00885 [astro-ph.CO]].
- [71] C. Yuan and Q. G. Huang, Phys. Lett. B **821** (2021), 136606 [arXiv:2007.10686 [astro-ph.CO]].
- [72] R. Jinno, T. Moroi and K. Nakayama, JCAP **01** (2014), 040 [arXiv:1307.3010 [hep-ph]].
- [73] C. Fu, P. Wu and H. Yu, Phys. Rev. D **101** (2020) no.2, 023529 [arXiv:1912.05927 [astro-ph.CO]].
- [74] S. Choudhury and A. Mazumdar, Phys. Lett. B **733** (2014), 270-275 [arXiv:1307.5119 [astro-ph.CO]].
- [75] S. Choudhury, S. Panda and M. Sami, Phys. Lett. B **845** (2023), 138123 [arXiv:2302.05655 [astro-ph.CO]].
- [76] S. Choudhury, S. Panda and M. Sami, JCAP **11** (2023), 066 [arXiv:2303.06066 [astro-ph.CO]].
- [77] S. Choudhury, S. Panda and M. Sami, JCAP **08** (2023), 078 [arXiv:2304.04065 [astro-ph.CO]].
- [78] G. Domènech, Universe **7** (2021) no.11, 398 [arXiv:2109.01398 [gr-qc]].
- [79] G. Domènech, Int. J. Mod. Phys. D **29** (2020) no.03, 2050028 [arXiv:1912.05583 [gr-qc]].
- [80] S. Balaji, G. Domènech and G. Franciolini, JCAP **10** (2023), 041 [arXiv:2307.08552 [gr-qc]].
- [81] M. Tagliazucchi, M. Braglia, F. Finelli and M. Pieroni, [arXiv:2310.08527 [astro-ph.CO]].
- [82] R. C. Bernardo and K. W. Ng, Phys. Rev. D **107** (2023) no.10, L101502 [arXiv:2302.11796 [gr-qc]].
- [83] R. C. Bernardo and K. W. Ng, JCAP **08** (2023), 028 [arXiv:2304.07040 [gr-qc]].
- [84] S. Appleby and R. C. Bernardo, JCAP **12** (2023), 003 [arXiv:2308.01712 [gr-qc]].
- [85] J. Li and G. H. Guo, Phys. Rev. D **107** (2023) no.4, 043536 [arXiv:2204.09237 [astro-ph.CO]].
- [86] J. Li and G. H. Guo, Eur. Phys. J. C **81** (2021) no.7, 602 [arXiv:2101.09949 [astro-ph.CO]].
- [87] J. Li, G. H. Guo and Y. Zu, Eur. Phys. J. C **84** (2024) no.10, 1083 [arXiv:2312.04589 [gr-qc]].
- [88] Z. C. Chen, J. Li, L. Liu and Z. Yi, Phys. Rev. D **109** (2024) no.10, L101302 [arXiv:2401.09818 [gr-qc]].
- [89] P. A. R. Ade *et al.* [BICEP2 and Keck Array], Phys. Rev. Lett. **121** (2018), 221301 [arXiv:1810.05216 [astro-ph.CO]].
- [90] N. Aghanim *et al.* [Planck], Astron. Astrophys. **641** (2020), A6 [arXiv:1807.06209 [astro-ph.CO]].
- [91] F. Beutler, C. Blake, M. Colless, D. H. Jones, L. Staveley-Smith, L. Campbell, Q. Parker, W. Saunders and F. Watson, Mon. Not. Roy. Astron. Soc. **416** (2011), 3017-3032 [arXiv:1106.3366 [astro-ph.CO]].
- [92] A. J. Ross, L. Samushia, C. Howlett, W. J. Percival, A. Burden and M. Manera, Mon. Not. Roy. Astron. Soc. **449** (2015) no.1, 835-847 [arXiv:1409.3242 [astro-ph.CO]].
- [93] S. Alam *et al.* [BOSS], Mon. Not. Roy. Astron. Soc. **470** (2017) no.3, 2617-2652 [arXiv:1607.03155 [astro-ph.CO]].

- [94] P. A. R. Ade *et al.* [BICEP and Keck], Phys. Rev. Lett. **127** (2021) no.15, 151301 [arXiv:2110.00483 [astro-ph.CO]].
- [95] A. Lewis and S. Bridle, Phys. Rev. D **66** (2002), 103511 [arXiv:astro-ph/0205436 [astro-ph]].